# A NOVEL MAGNETICALLY METHOD PLANNING TO FETUS HEART RATE MONITORING WITHOUT SIDE EFFECTS

Kourosh Mousavi Takami[1], Homa Hekmat[2]

[1] TDI researcher, ACECR, IRI; [2] Assistant in obstetrics and genecology

Corresponding Author: K.M. Takami, No 112, Almogelpl 13, 724 80, Västerås, Sweden;
Kourosh.mousavi.takami@mdh.se, homahekmat@yahoo.com

**Abstract**. At present, the most common way of diagnosing fetal heart ailments is through an ultrasound examination. While ultrasound can reveal the shape of the heart and provide some information about the working of the heart and blood flow, it is unable to provide the type of electrophysiological information directly related to cardiac activity that is furnished by an electrocardiogram or magnetocardiogram. Attempts have been made to obtain electrocardiograms from the fetal heart using electrodes placed on the mother's abdomen or using the surface touch of solenoids and receiver devices. However, the electrical fields emitted by the fetal heart are so minute that it is difficult to separate them from the electrical signals generated by the mother's heart.

Based of individual researcher reports, there are indeed some potential dangers to the fetus in administring ultrasound tests. They are: "Postnatal thermal effects, fetal thermal effects, postnatal mechanical effects, fetal mechanical effects, and bioeffects considerations for ultrasound contrast agents. Ultrasound energy produces a mechanical pressure wave through soft tissue. This pressure wave may cause microscopic bubbles in living tissues, and distortion of the cell membrane, influencing ion fluxes and intracellular activity. When ultrasound enters the body, it causes molecular friction and heats the tissues slightly. This effect is very minor as normal tissue perfusion dissipates heat. With high intensity, it can also cause small pockets of gas in body fluids or tissues to expand and contract/collapse in a phenomenon called cavitation (this is not known to occur at diagnostic power levels used by modern diagnostic ultrasound units). The long-term effects of tissue heating and cavitation are not known.

According to mentioned side effects, it needs to design a new device to fetus heart rate measuring without dangerous. It has proved that human organs make poor magnetic fields. In the fetal magnetocardiography method the magnetic activity of the fetal heart is measured. Fetal magnetocardiography (F-MCG) is a non-invase technique in which the magnetic field caused by electrical activity within the fetal heart is measured.

Consequently, using robust sensors, equipped apparatuses, power full software and algorithm fetus heart rate should be simulated and compared with test results to validate of defined heart model. This research will present a new and beneficial method to monitor of fetus heart rate without any side effects. As the mentioned above, due to ultrasonic wave's problem this method can be used in fetus heart rate monitoring. Non stress test and other showed methods can not compete with this healthy method.

## 1    Introduction

As of May 23, 2008, the AIUM published an article called "American Institute of Ultrasound in Medicine Consensus Report on Potential Bio effects of Diagnostic Ultrasound: Executive Summary" stating that there are indeed some potential dangers to the fetus in administring ultrasound tests. They are: "Postnatal thermal effects, fetal thermal effects, postnatal mechanical effects, fetal mechanical effects, and bioeffects considerations for ultrasound contrast agents."[1] Ultrasound energy produces a mechanical pressure wave through soft tissue. This pressure wave may cause microscopic bubbles in living tissues, and distortion of the cell membrane, influencing ion fluxes and intracellular activity. When ultrasound enters the body, it causes molecular friction and heats the tissues slightly. This effect is very minor as normal tissue perfusion dissipates heat. With high intensity, it can also cause small pockets of gas in body fluids or tissues to expand and contract/collapse in a phenomenon called cavitation (this is not known to occur at diagnostic power levels used by modern diagnostic ultrasound units). The long-term effects of tissue heating and cavitation are not known.[2] There are several studies that indicate the harmful side effects on animal fetuses associated with the use of sonography on pregnant mammals. A noteworthy study in 2006 suggests exposure to ultrasound can affect fetal brain development in mice. This misplacement of brain cells during their development is linked to disorders ranging "from mental retardation and childhood epilepsy to developmental dyslexia, autism spectrum disorders and schizophrenia, the researchers said. However, this effect was only detectable after 30 minutes of continuous scanning. [3] A typical fetal scan, including evaluation for fetal malformations, typically takes 10-30 minutes.[4] There is no link made yet between the test results on animals, such as mice, and the possible outcome to humans. Widespread clinical use of diagnostic

ultrasound testing on humans has not been done for ethical reasons. The possibility exists that biological effects may be identified in the future, currently most doctors feel that based on available information the benefits to patients outweigh the risks.[5] Obstetric ultrasound can be used to identify many conditions that would be harmful to the mother and the baby. For this reason many health care professionals consider that the risk of leaving these conditions undiagnosed is much greater than the very small risk, if any, associated with undergoing the scan. According to Cochrane review, routine ultrasound in early pregnancy (less than 24 weeks) appears to enable better gestational age assessment, earlier detection of multiple pregnancies and earlier detection of clinically unsuspected fetal malformation at a time when termination of pregnancy is possible.

There is great interest in using high-Tc Superconducting Quantum Interference Device (SQUID) magnetometers for biomagnetic applications to examine the heart. One of the most important issues for the SQUID magnetometer is how to improve the magnetic field sensitivity.

To improve the sensitivity, the magnetic field sensing area needs to be increased, and the noise of the SQUID in the interesting frequency band should be reduced as much as possible. To increase the effective sensing area, the best way is to integrate SQUIDs with multi-turn input coils connected to large pick-up loops. However, it is not easy to fabricate multi-turn input coils, because the multi-level process for oxide films has not been fully optimized yet.

SQUID magnetometers with good noise properties can be obtained by using ip-chip coupling of a SQUID to a ux transformer consisting of an input coil connected to a large pick-up coil. However, this is not desirable for producing the large number of SQUIDs needed for multi-channel SQUID systems. Hence, the easiest way to increase the effective sensing area is to make a \directly coupled SQUID" which needs only a single-layer superconducting thin film, though it is not the most effective method. In a directly coupled SQUID, a large pick-up loop is coupled to a SQUID washer on the same thin film layer.

Obstetric ultrasound can be used to identify many conditions that would be harmful to the mother and the baby. A noteworthy study in 2006 suggests exposure to ultrasound can affect fetal brain development in mice. This misplacement of brain cells during their development is linked to disorders ranging "from mental retardation and childhood epilepsy to developmental dyslexia, autism spectrum disorders and schizophrenia, the researchers said. However, this effect was only detectable after 30 minutes of continuous scanning.

As the magnetic fields over the maternal abdomen are tiny, superconducting devices are used to record these fields. Presently, these measurements are conducted in a magnetically shielded room, because fetal cardiac signals have only a very small magnitude. The very low magnetic fields are measured with liquid Helium cooled SQUID sensors. In the shielded room, the achieved white noise level is typically 10 fT/sqrt Hz while the peak magnetic field of the fetal heart is about about 2-30 pT (= $0.2$-$3\times10^{-11}$ T), when measured above the maternal abdomen.

Using a SQUID-based sensor enables the weak magnetic fields generated by the fetal heart to be measured by placing the sensor on the mother's abdomen. Measurements obtained with this method are virtually unaffected by the amniotic fluid or fetal fat, making it possible to obtain signals with a higher resolution than an electrocardiogram.

A new sensor was developed that reduces the influence of the mother's myocardial magnetic field on the measurements and makes it possible to accurately measure the cardiac magnetic field of the fetus. The fetus's heart is normally about 6 cm from the surface of the mother's abdomen, so the new sensor was developed with a high sensitivity that, compared to a conventional sensor, gives it more sensitivity at a deeper depth. The new procedure can also be used to perform separate measurements on twins.

Fetal electrocardiograms can be obtained as early as the twentieth week of pregnancy. Thus, the new procedure should make possible the early detection of fetal cardiac ailments, and thereby facilitate treatment of the condition, either before or immediately after birth.

Powerful Multiphysics software like COMSOL environment for modelling and solving all kinds of problems based on partial differential equations (PDEs) has been used in this study. With this software authors easily extend physics of heart model into multiphysics models that solved coupled physics phenomena and do so simultaneously. Using this software with in-depth knowledge of mathematics or numerical analysis simulation of fetus heart in the many kinds of model like electromagnetic fields, acoustic, fluid dynamic, heat transfer and fluid thermal interactions has been performed. With built of model in software physics mode it is possible to build models by defining the relevant physical quantities—such as material properties, loads, constraints, sources, and fluxes rather than by defining the underlying equations. It can always apply these variables, expressions, or numbers directly to solid domains, boundaries, edges, and points independently of the computational mesh. COMSOL Multiphysics then internally compiles a set of PDEs representing the entire model. It accesses the power of COMSOL Multiphysics as a standalone product through a flexible graphical user interface, or by script programming in the COMSOL Script language or in the MATLAB language. This capability shows this software ability to simulate of proposed heart model to find the fetus heart rate.

In the fetal heart monitor this technique is improved to be applied outside the shielded room in a standard clinical environment. The goal of this research is to demonstrate the functionality of an F-MCG measurement system that contains two major improvements:

- A non harmful device theoretical analyzing to fetal heart rate monitoring with user friendly cooling system that is enclosed in a small box besides the patient, with a sensor head that can be positioned above the patient.

- A new noise reduction system that separates the fetal MCG signal form the environmental noise in a regular (=unshielded) environment

Developed a SQUID based magnetic-detection system for fetal magneto-cardiography (fetal MCG) with a dedicated cooling system that can be operated without a magnetically shielded room. The SQUID sensors are located in a measuring head and cooled by circulating helium that, in turn, is cooled by a cryocooler placed at a distance of ~1.5m from the measuring head. The interference from the coolers requires them to be separated from the sensor head. The measuring head can be rotated to allow for a movement to the position above the patient where the best signal can be obtained.

Recently, it obtained the first preliminary results after a successful cool down of the system down to an operating temperature of 4.5 Kelvin, for the SQUID and gradiometers. Measured Magneto Cardio-Gram (MCG) of the adult heart in real time with a bandpass filter and 50Hz noise suppression in real time:
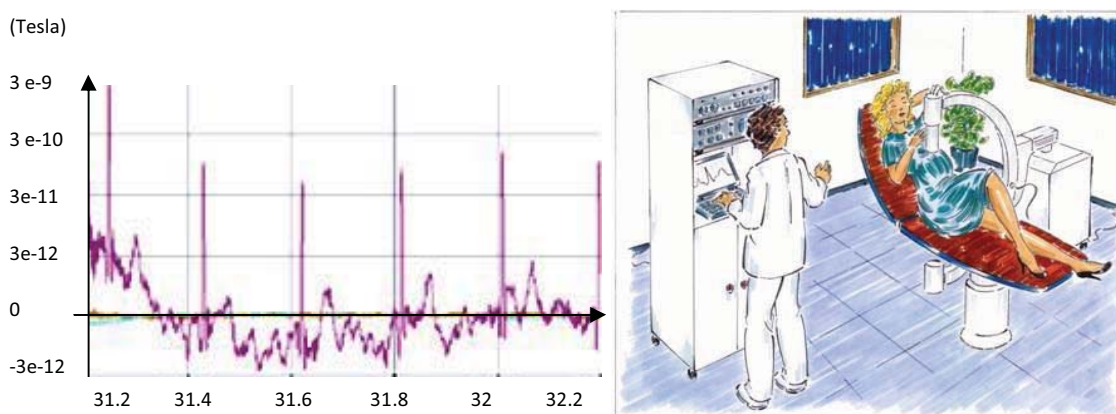


**Figure1.** Artist impression of a future fMCG measurement setup; real time Magneto Cardio-Gram (MCG) of an adult hears

Averaging this result ~150 times gives a very clear MCG of the subject with an amplitude of approximately 30pT, measured in a regular lab/office environment.

## 2 Non stress test

Before mention about F-MCG need to describe on NST test that is a competitor of this test, today. The nonstress test (NST) uses a fetal heart rate monitor to observe the heart rates of babies. The NST is considered reactive (normal) when the babies' heart rates increase fifteen beats per minute, two times during twenty minutes. A non reactive (abnormal) NST is noted if there are decreases in the babies, heart rates or no increases with their movements. This can mean babies' receiving enough oxygen because of cord compression, low amniotic fluid levels, or poor placental function. However, lack of activity can mean that one or more babies are in normal sleep cycle. Some doctors use fetal acoustic simulation (FAS) to waken sleepy babies so that they are more responsive. With FAS, an artificial larynx or other sound devices is placed on a mother's abdomen and activated for a few seconds. Sometimes the movement of one baby is enough to simulate the others. Studies have found no hearing loss in children exposed to FAS during pregnancy. It is thought that the amniotic fluid and the fluid inside the middle are help muffle the sound.

Nonstress testing is often used to monitor babies who have poor growth, twin-to-twin transfusion syndrome(TTTS), or placental problems, or when mother has gestational diabetes. In late pregnancy, NSTs might be done frequently to watch for signs that the placentas are going or not functioning effectively. A non reactive NST may require the preterm delivery of babies. The NST can be done as early as the 27th week of pregnancy.

Another related test is contraction stress test (CST). This test uses medication such as pitocin or simulation of the mother's nipples to cause contractions. The babies' responses to the contractions are monitored for signs of distress. Because of the risk of preterm labor with multiples, the CST is not commonly used. Often, a spontaneous CST can occur when a mother has a contraction on her own during an NST, and the babies' response can be documented. Figure 2 shows the monitored and graphed cases of NST. One of the main problems in NST is related to understand of ripple and curves by MD doctors.
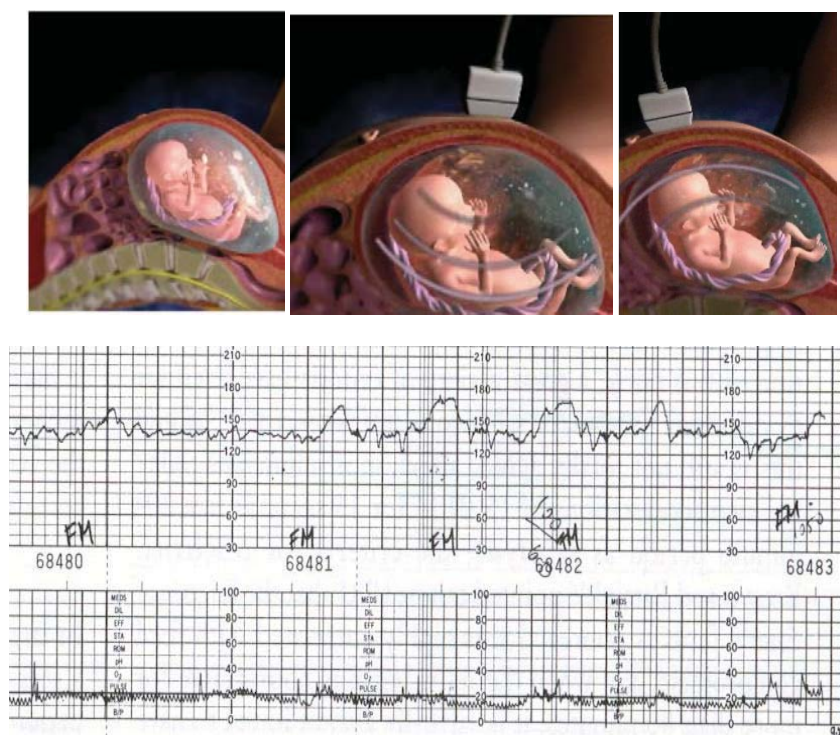
**Figure 2:** Nonstress test mentoring and recorded results

## 3 Magnetocardiography

Fetal magnetocardiography, a technique recording the magnetic field generated by the electrical activity of the fetal heart rate, offers a more precise delineation of the fetal electrophysiology. Detection occurs non-invasively by sensors cooled by liquid helium positioned several centimeters above the maternal abdomen in a magnetically shielded room. As the maternal heart generates magnetic activity as well, a maternal ECG is recorded simultaneously and substracted from the fetal MCG. This way, an averaged one lead fetal MCG is obtained and allows for a more detailed differentiation of the type of tachycardia.

Magnetocardiography is the measurement of magnetic fields emitted by the human heart from small currents by electrically active cells of the heart muscle. The measurement of these fields over the torso provides information which is complementary to that provided by electrocardiography, used especially in diagnosing abnormalities of heart function.

Fetal electrocardiograms can be obtained as early as the twentieth week of pregnancy. Thus, the new procedure should make possible the early detection of fetal cardiac ailments, and thereby facilitate treatment of the condition, either before or immediately after birth.

### 3.1 Sensor to detect magnetic field

A tiny sensor that can detect magnetic field changes as small as 70 femtoteslas equivalent to the brain waves of a person daydreaming has been demonstrated at the National Institute of Standards and Technology (NIST). The sensor could be battery operated and could reduce the costs of non-invasive biomagnetic measurements such as fetal heart monitoring. The device also may have applications such as homeland security screening for explosives.

The prototype device is almost 1000 times more sensitive than NIST's original chip-scale magnetometer demonstrated in 2004 and is based on a different operating principle. Its performance puts it within reach of matching the current gold standard for magnetic sensors, so-called superconducting quantum interference devices or SQUIDs. These devices can sense changes in the 3- to 40-femtotesla range but must be cooled to very low (cryogenic) temperatures, making them much larger, power hungry, and more expensive.

The NIST prototype consists of a single low-power (milliwatt) infrared laser and a rice-grain-sized container with dimensions of 3 by 2 by 1 millimeters. The container holds about 100 billion rubidium atoms in gas form. As the laser beam passes through the atomic vapor, scientists measure the transmitted optical power while varying the strength of a magnetic field applied perpendicular to the beam. The amount of laser light absorbed by the atoms varies predictably with the magnetic field, providing a reference scale for measuring the field. The stronger the magnetic field, the more light is absorbed.

The new sensor is already powerful enough for fetal heart monitoring; with further work, the sensitivity can likely be improved to a level in the 10 femtotesla range, sufficient for additional applications such as measuring brain activity,

the designers say. A femtotesla is one quadrillionth (or a millionth of a billionth) of a tesla, the unit that defines the strength of a magnetic field. For comparison, the Earth's magnetic field is measured in microteslas, and a magnetic resonance imaging (MRI) system operates at several teslas.

To make a complete portable magnetometer, the laser and vapor cell would need to be packaged with miniature optics and a light detector. The vapor cell can be fabricated and assembled on semiconductor wafers using existing techniques for making microelectronics and microelectromechanical systems (MEMS). This design, adapted from a previously developed NIST chip-scale atomic clock, offers the potential for low-cost mass production.

NIST scientists demonstrated that the prototype mini-sensor produces a strong signal that changes rapidly with the strength of a magnetic field from the outside world. The device exhibits a consistent minimum level of electromagnetic static, or "white noise," which indicates a stable limit on its overall sensitivity. The authors also estimate that a well-designed compact magnetometer with present sensitivity could operate continuously for weeks on a single AA battery. Magnetometers need to be designed with applications in mind; smaller vapor cells require less power but are also less sensitive. Thus, an application for which low power is critical would benefit from a very small magnetometer, whereas a larger magnetometer would be more suitable for a different application requiring high sensitivity.

The NIST device could be used in a heart monitoring technique, magnetocardiography (MCG), which is sensitive enough to measure fields of few picoteslas emitted by the fetal heart from small currents in heart muscle cells, providing complementary and perhaps better information than an electrocardiogram.

### 3.2 Magneto-cardiogram of the Fetal heart rate

The magnetic fields that are presently used in medicine range from ~1.5 Tesla, in a Magnetic Resonance Imaging (MRI) system, down to ~1 femto-Tesla (1 fT = $10^{-15}$ T), which is a typical detection limit in a Magneto-EncephaloGram (MEG) system measuring the activity of a human brain. The field present in an MRI-system is approximately 30,000× as strong as the naturally present magnetic field of the earth of ~50 micro-Tesla (50 µT = $50×10^{-6}$ T). Compared to this field, the magnetic signals measured around our head are extremely small, typically 0.000,000,000,000,5× the magnetic field of the earth.

The broad magnetic field-range applied medicine explains why the Biomag group is part of the Low Temperature division. To generate a magnetic field sufficiently strong for MRI and to measure a magnetic signal sufficiently sensitive for MEG, superconducting systems are required. Superconducting devices can only be operated at temperatures far below room temperature. At present almost all MRI and MEG systems placed in hospitals are operated at a temperature near 4 Kelvin (= -269 ºC).

In the fetal magnetocardiography the magnetic activity of the fetal heart is measured. Fetal magnetocardiography (F-MCG) is a non-invase technique in which the magnetic field caused by electrical activity within the fetal heart is measured. As the magnetic fields over the maternal abdomen are tiny, superconducting devices are used to record these fields. Presently, these measurements are conducted in a magnetically shielded room, because fetal cardiac signals have only a very small magnitude. The very low magnetic fields are measured with liquid Helium cooled SQUID sensors. In the shielded room, the achieved white noise level is typically 12 fT/sqrt Hz while the peak magnetic field of the fetal heart is about 0.2-0.3pT (= $2-3×10^{-11}$ T), when measured above the maternal abdomen.
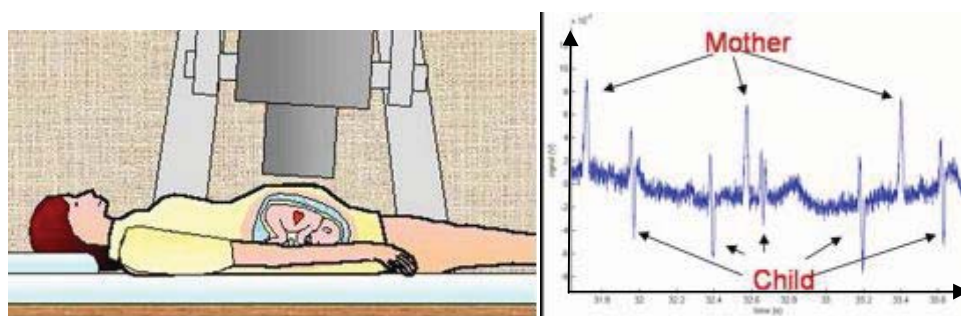


**Figure 3**. The planned F-MCG measurement setup placed above the patient. The graph shows the measured MCG signal (mother and child) [6].

Before of simulation a case study on fetus magnetic field with age dependency has been performed, on 93 cases. Results that discussed in the following showed that with increasing of fetus age, magnetic fields of fetus heart increased. See tables 1 and 2. F-MCG was acquired at a sampling rate of 1 KHz in each case. A 0.1-200-Hz band-pass filter and a 50-Hz power-line noise filter were applied. Immediately before F-MCG recording, the shortest distance from the maternal abdominal surface to the anterior ventricular surface of the fetal heart ($d_1$) was determined. A view of the four cardiac chambers on fetal echocardiograms was also used to identify any structural cardiac abnormalities as well as to measure TCD. F-MCG was recorded simultaneously at nine points for at least 2 min by placing the sensor array as close as possible to the maternal abdominal surface. When the maximum point was not at the center of the first

mapped area and was suspected to be out of the area from the magnetic distribution pattern, the sensor array was moved a few centimetres until the peak value was detected. No less than 20 beats with the maximum amplitude and the same polarity of the waveform were selected from the tracings among nine channels. Then, signal averaging of the data triggered by the peak of the QRS complex was applied to improve the signal-to-noise ratio. According to the methods described by Williamson and Kaufman, the magnitude of the one-current dipole of the fetal heart was calculated, based on the data of F-MCG and depth of the fetal heart, using the following equation: where $d_1$ is the distance between the sensor coil and fetal ventricular wall, $\mu_0$ is a constant of the magnetic permeability, B is the normal (z) component of the maximum magnetic force during ventricular depolarization among nine channels, and Q is the current dipole to be estimated. For a first-order gradiometer with baseline L (60 mm in the present system), equation (a) can be transformed into the following equation (b): Thus, MATH where $d_2 = d_1 + L$. $B = \frac{0.385\mu_0}{4\pi d_1^2} Q$    Equation 1, a; $Q = \frac{4\pi B}{0.385\mu_0}\left(\frac{1}{d_1^2} - \frac{1}{d_2^2}\right)^{-1}$ Equation 2, b, $B = \frac{0.385\mu_0}{4\pi}\left(\frac{1}{d_1^2} - \frac{1}{d_2^2}\right) Q$    Equation 3, c.

Consequently, the magnitude of the current dipole (Q) is simply estimated using two parameters, *i.e.* the maximum magnetic force measured on the maternal abdomen (B) and the depth of the fetal heart determined by fetal echocardiography ($d_1$). The correlation of B and Q values with gestational age was analyzed using simple linear regression.

| Gestation | NOC | $d_1$(mm)* | B(pico T) | Q(nAm) |
|---|---|---|---|---|
| <28wk | 15 | 41.3±7.8 | 2.77±0.8 | 146±461.08 |
| 28-31wk | 20 | 42.3±9.6 | 3.38±1.13 | 207±86.7 |
| 32-35wk | 19 | 44.6±11.8 | 4.29±2.15 | 237.2±109 |
| >35wk | 32 | 47.8±11.5 | 4.45±1.61 | 293.8±138 |

| Biomagnetic fields | Human heart | Fetal heart | human eye | Human brain |
|---|---|---|---|---|
| Tesla | $2*10^{-10}$ | $3*10^{-11}$ | $7*10^{-12}$ | $8*10^{-13}$ |

**Table1.** Maximum amplitude of fMCG measured on maternal abdomen ( B) and estimated magnitude of the current dipole ( Q ) in normal fetuses.
Values are expressed as mean ±SD; *Depth of the fetal heart determined by fetal echocardiography; NOC: no. of cases.

| Case no. | Gestation (wk-d) | Cause of cardiomegaly | TCD (mm) | Q (nAm) |
|---|---|---|---|---|
| 1 | 23-2 | TTS | 31.5 | 311 |
| 2 | 26-1 | TTS | 37 | 362 |
| 3 | 30-1 | Galen | 43 | 409 |
| 4 | 32-3 | ECD | 44.6 | 552 |
| 5 | 33-1 | TTS | 45.8 | 289 |
| 6 | 33-1 | ECD | 45.8 | 623 |
| 7 | 36-4 | Galen | 55 | 1332 |

**Table2.** Measurements of TCD and estimated magnitude of the current dipole (Q) in fetuses with cardiomegalyTTS, twin-twin transfusion syndrome; Galen, malformation of the vein Galen; ECD, endocardial cushion defect.
TTS: twin-twin transfusion syndrome; Galen, malformation of the vein Galen; ECD, endocardial cushion defect.

### 3.3  Generation of the MCG signal from the electric activation of the heart

As mentioned earlier, the source of the MCG signal is the *electric* activity of the heart muscle. The generation of the MCG signal from the progress of the activation front in the heart can be sketched similarly with the aid of the MCG lead fields.

In Figure 4 the generation of the MCG signal in the *x* and *z* leads is sketched. This illustration is only a rough approximation, and its purpose is to give an impression of the principle of how the signal is produced. As regards the *x* component, it is assumed that because of the strong proximity effect, the signal is generated mainly from the activation in the anterior part of the heart. As regards the *z* component, it is pointed out that in nonsymmetric unipositional MCG measurements the zero sensitivity line is located in the posterior side of the heart. Because the sensitivity is proportional to the distance from the zero sensitivity line, the contribution of the anterior part of the heart is again dominating.
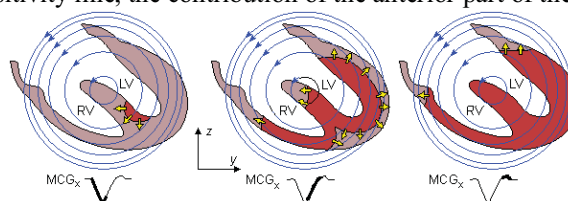


**Figure. 4.**  Schematic illustration of the generation of the x component of the MCG signals.

Magneto cardiography non-invasive registers the magnetic component of cardiac electric activity. Figure 5, 6 and 7 shows the simulation of magnetic fields in mother abdomen with fetus placed there. These shown the filed contour and distribution in mother abdomen and around of her body due to heart, brain, eyes and etc. Figures 8 and 9 shows magnetic field on curves in the fetus and the maternal, these MCG signals found by simulation. Subjects were in a resting, supine condition.

Data were recorded at a sampling rate of 1 kHz and a band pass of 1–200 Hz. With figure outing the result from figure 8, shows that the fetus and mother heart rate in straight distance on the mother abdomen is greater than other part.
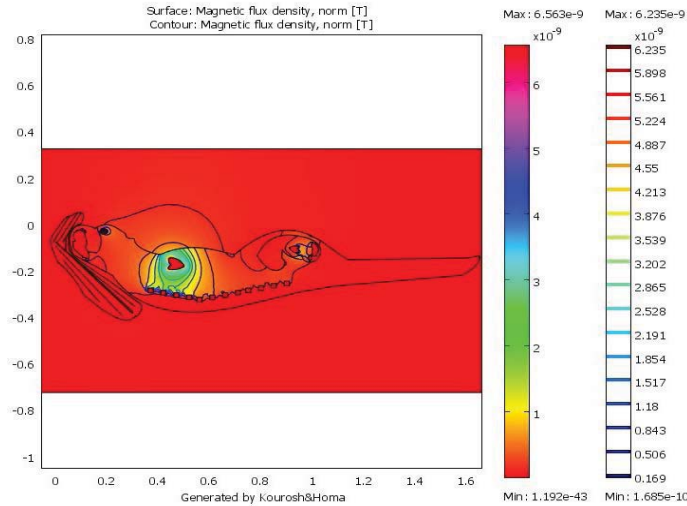


**Figure5.** Mother's along with fetus magnetic flux density propagations
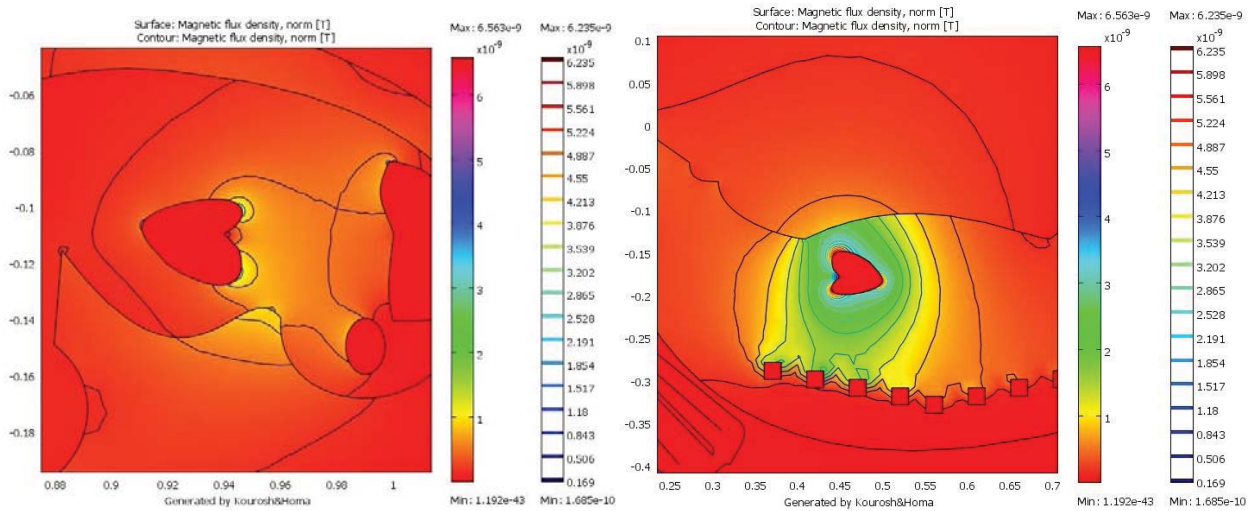


**Figure 6.** Fetus magnetic flux density propagations    **Figure 7.** Mother's magnetic flux density propagations
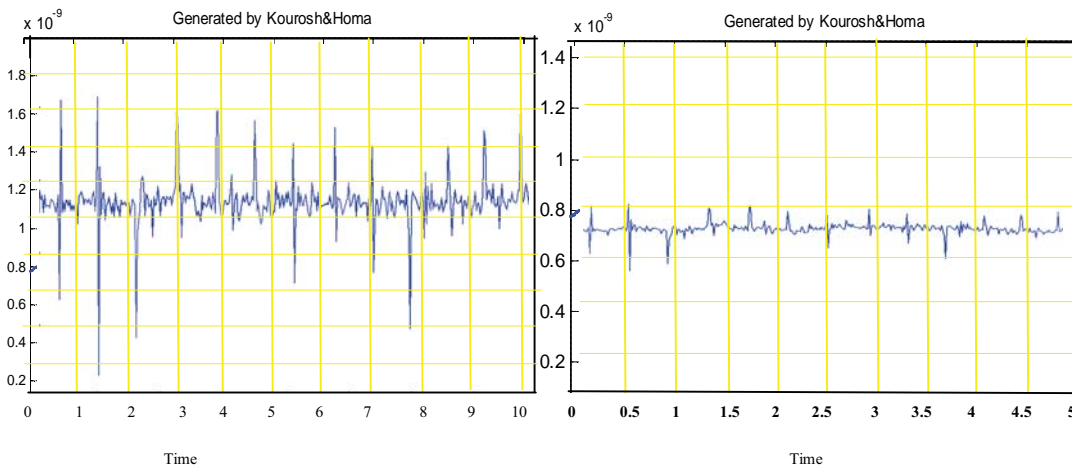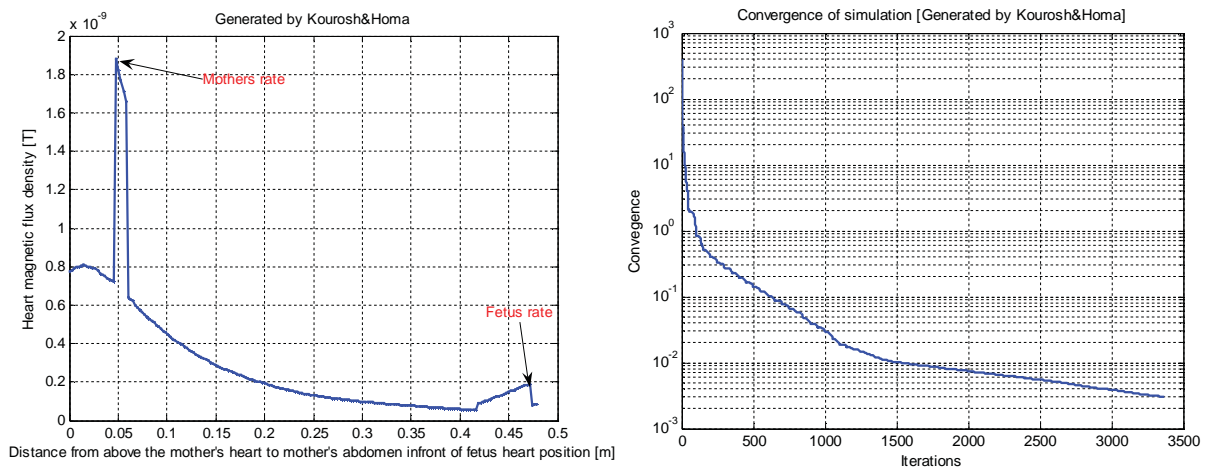
**Figure 8.** The heart rhythm of mother and fetus in 31 weeks of pregnancy

Distance of the heart by mother abdomen skins, electric conductivity and magnetic permeability's of tissues, noise rate, other organs activities, stress of mother in during of test, nervous activities, mother's contractions, blood and other organs electric and magnetic properties have the main effects on simulation results. Other main parameter is related to the fetus placing in the mother abdomen. His/her face and heart is in top or bottom towards of mother position, each one's have the different effects on the results. Simulation shows that the mother heart rate is around of 2e-8 Tesla in maximum rate and is less than 2e-9 for fetus in maximum rate. This values change after noise processing to 1.6e-9 for mother heart rate and 8e-10 for fetus heart rate in Tesla unit.

Other main parameter in fetal heart rate monitoring is age of fetus. This is an important question, which month is the optimum month to monitoring. It seems 10-27 weeks is a reasonable age but author are analyzing and researching to find the proper month of pregnancy for monitoring of heart rate. Figure 9 shows the variation of frequency and magnitude of fetal heart rate in different pregnancy times.
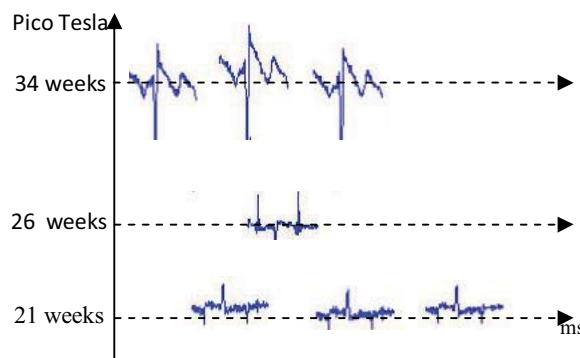


**Figure 9.** Simulated maternal and fetus heart rate

Simulation has been performed in Comsol and Matlab soft wares using ordinary governing equation but it still needs to verifications. To verify of claim used the Echo and Doppler test that has been performed by other researcher, it put to judge of simulation results. With look at to figure 10, the negative Doppler velocities characterize inflow during diastole across the tricuspid valve; the positive velocities characterize systolic outflow into the pulmonary artery. Above the Doppler tracing is a timing signal recorded through the scanner's ECG input (grey) and through the F-MCG data acquisition system (white and opposite polarity), which is used to align the Doppler and the F-MCG. The timing signal is square, but is distorted by high-pass filtering. The amplitude of the QRS complex in the F-MCG is approximately 3e-9 Tesla. It shows the best fit of results, it seems simulation have a good results. These are proved and validated by figures 2 and 10. In figure 2 NST results recorded and shown the amplitude about nano to femto Tesla.

## 4    Signal Analysis

In the raw data of the MCG signal, templates of both the maternal and fetal QRS complex were formed using 7 representative complexes (maternal and fetal, respectively) with a high signal to noise ratio. The fetal and the maternal R peaks were identified to an accuracy of 1 ms on the basis of the correlation to these respective QRS signal templates (see also Fig. 9). Figure 11 shows the block diagram of signal processing and noise removing system. This system used from adaptive noise cancelling system with two input signal, first is the main signal and other one is a reference input.

The reference input has been obtained by simulation result that sent to work space of Matlab software. The reference noise signal input obtains acquisition of $x_n$, according to predicting the square of error and minimum criterion. First the author estimated the step of AR model of the auto-regression prediction filtering, and then predicted the coefficient of AR model of the auto-regression prediction filtering through the Levinson-Durbin algorithm. The predicting reference passway signal act as the noise signal estimated value of main input in order to offset the noise signal from main channel and realize the abstraction of the Fetal Heart Rate signal. The author adopted the transversal filter in the adaptive filter of the adaptive noise cancelling system. The algorithm of clipped-error LMS with variable step size of segmenting type was adopted, through computer simulation experiment, SNR improved about 30db. the author realized the abstraction of Fetal Heart Rate signal and proved its validity and superiority.

Using the timing of the R peaks, fetal and maternal RR interval time series were constructed and the timing of the R peaks of the one time series in relation to each RR interval of the other time series was noted. The relative timing of the fetal (or maternal) R peak with respect to the simultaneous maternal (or fetal) RR cycle is referred to in the following as the phase $\varphi_{mat}$(or $\varphi_{fet}$).
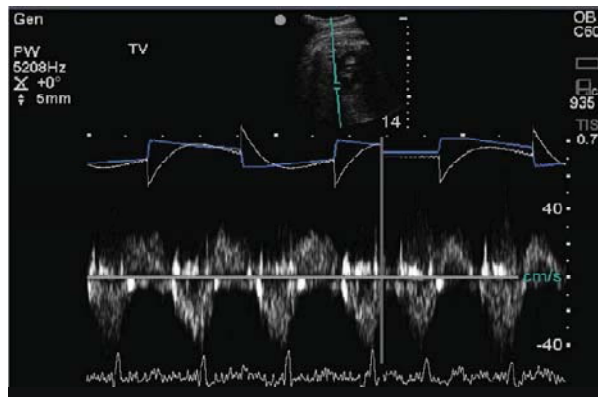


**Fiure10.** Echo and Doppler registered of right ventricular inflow and outflow showing synchronized F-MCG in the bottom tracing.
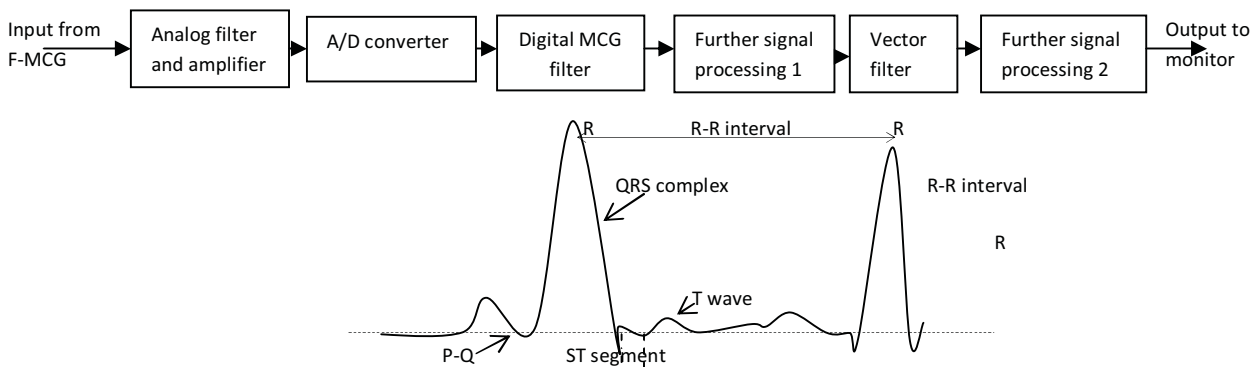


**Figure11**: signal processing and noise filtering block diagram of F-MCG

### 4.1 Method and noise formulation

Here formulate a linear minimum mean-square error (LMMSE) filter and show that it can significantly improve the SNR of fetal heart magnetic rate response (FMCG) data.

Let X denote a n$\times T$ data matrix representing a single trial, where n is the number of channels and T is the number of samples in each trial. Suppose S and N denote the signal and noise, respectively, so X = S + N. Define the mean-square error (MSE) between the signal and the spatial filter, F, applied to the data as: $e^2(F) = \langle(S - FX)(S - FX)'\rangle$. The filter that minimizes $e^2(F)$ is given by F = $F_{min}$ = $R_{ss}R_{xx}^{-1}$ where $R_{ss}$ = $\langle SS'\rangle$ and Rxx = $\langle XX'\rangle$. The minimum MSE is: $e_{min}^2 = tr\{R_{ss} - R_{ss}R_{xx}^{-1}R_{ss}\}$. In practice, $R_{SS}$ and $R_{XX}$ are not available and must be approximated using the data. Let X1;X2; . . . ;XJ denote J independent trials in a multiepoch recording and assume Xi = Si +Ni. It is straightforward to approximate $R_{XX}$ using the sample average: $\hat{R}_{xx} = \frac{1}{J}c$.

For J large enough, we have $\hat{R}_{xx} \to$ Rxx. We exploit the mean of the signal and noise to approximate RSS as $\hat{R}_{xx} = X_{ave}X_{ave}^t$ . Where $X_{ave} = \frac{1}{J}\sum_{i=1}^{j} X_i$. The mean of $\hat{R}_{ss}$ is $\langle\hat{R}_{xx}\rangle = \bar{S}\bar{S}^t + \frac{1}{J}C_s + \frac{1}{J}C_N$. Where $\bar{S} = \langle S\rangle$ Note that $\hat{R}_{ss}$ is biased since the quantity we seek to approximate is $R_{ss} = \bar{S}\bar{S}^t + C_s$.

The excess MSE, $e_{ex}^2(F) = e^2(F) - e_{min}^2$ can be expressed as: $e_{ex}^2(F) = tr\{(F - R_{ss}R_{xx}^{-1})Rxx(F - R_{ss}R_{xx}^{-1})^t\}$.

For this analysis we assume that J is sufficiently large so that $\hat{R}_{ss}$ and $\hat{R}_{xx}$ approach $\langle \hat{R}_{ss} \rangle$ and RXX, respectively, and thus use $F_{a_{pp}} = \langle \hat{R}_{ss} \rangle R_{xx}^{-1}$ to compute the excess MSE in place of $\hat{F}$. This yields $e_{ex}^2(F_{a_{pp}}) = tr\left\{ \left( \frac{J-1}{J} C_s - \frac{1}{J} C_N \right) \times R_{xx}^{-1} \left( \frac{J-1}{J} C_s - \frac{1}{J} C_N \right)^t \right\}$. which suggests $e_{ex}^2(F_{a_{pp}})$ decreases as CS decreases and J increases. We further consider the performance of $F_{a_{pp}}$ for the specific case of a rank-one signal $S = h \propto^t$, where h is an n×1 spatial pattern and $\propto$ is a T×1 random vector describing the time evolution of the signal. We assume $hh^t = 1$ and define $\bar{\propto} = \langle \propto \rangle$ and $\sigma^2 = \langle (\propto - \bar{\propto})^t (\propto - \bar{\propto}) \rangle$ and $\beta = \bar{\propto}^t \bar{\propto} + \sigma^2$. Note that with these definitions Rxx $= \beta hh^t + C_N$ and thus $R_{xx}^{-1}$ XX can be computed in closed form via the matrix inversion lemma.

We use the SNR of the estimated mean signal, $\widehat{\bar{S}} = F X_{ave}$, as a performance metric. First, note that $F_{min} X_{ave} = R_{ss} R_{xx}^{-1} \left( \bar{S} + \frac{1}{J} \sum_{i=1}^{j} (S_i - \bar{S}) \right) + \frac{1}{J} \sum_{i=1}^{j} N_i$ The power in $F_{min} X_{ave}$ due to the signal is defined as $SP(F_{min} X_{ave}) = tr\left\{ R_{ss} R_{xx}^{-1} \langle \left( \bar{S} + \frac{1}{J} \sum_{i=1}^{j} (S_i - \bar{S}) \right) \times \left( \bar{S} + \frac{1}{J} \sum_{i=1}^{j} (S_i - \bar{S}) \right)^t \rangle R_{ss} R_{xx}^{-1} \right\}$. Then: The noise power $= \beta^2 \gamma (\frac{v}{1+\beta v})^2$. Where $\gamma = \bar{\propto}^t \bar{\propto} + (\frac{1}{J}) \sigma^2$, $v = h C_N^{-1} h^t$. The noise power $NP(F_{min} X_{ave})$ in $F_{min} X_{ave}$ is defined similarly to obtain $NP(F_{min} X_{ave}) = \frac{1}{J} \beta^2 \frac{v}{(1+\beta v)^2}$.

Hence, the SNR of $F_{min} X_{ave}$ is: $SNR(F_{min} X_{ave}) = J \gamma v$. For comparison, the SNR of the mean in the absence of spatial filtering (F = I) is: $SNR(X_{ave}) = \frac{J\gamma}{tr\{C_N\}}$.

The ratio of the optimum spatial filter SNR to the SNR without spatial filtering is: $\frac{SNR(F_{min} X_{ave})}{SNR(X_{ave})} = v. tr\{C_N\}$. It can be shown that this rate is greater than one, so the optimum spatial filter always improves SNR. It can be shown that the SNR of $F_{a_{pp}} X_{ave}$ is $SNR(F_{a_{pp}} X_{ave}) = \dfrac{\gamma \left( \gamma + \frac{1}{J} v^{-1} \right) v^2}{\frac{1}{J} \gamma^2 v + \frac{1}{J^2} 2\gamma(1+\beta v) + \frac{1}{J^3}(tr\{C_N\} - \frac{2\beta + \beta^2 v}{1+\beta v})(1+\beta v)^2}$ and consequently: $\dfrac{SNR(F_{a_{pp}} X_{ave})}{SNR(X_{ave})} = \dfrac{\gamma \left( \gamma + \frac{1}{J} v^{-1} \right) v^2. tr\{C_N\}}{\gamma(\gamma^2 v + \frac{1}{J} 2\gamma(1+\beta v) + \frac{1}{J^2}(tr\{C_N\} - \frac{2\beta + \beta^2 v}{1+\beta v})(1+\beta v)^2}$ and when $J \to \infty$ this equation will be $v. tr\{C_N\}$.

The purpose of the simulations was to quantify the improvement in SNR and to assess the distortion of the spatial pattern introduced by the filter. the noise was an artificially generated white Gaussian noise time-series. A run of 400 trials was simulated by adding the synthetic signal to 400 1-s epochs of noise, with the peak of the synthetic signal positioned at time 0.22 s. result used to design of spatial filter that improve the SNR. Figure 11 and 12 shows its block.

## 1.1  Data Analysis

Several approaches were used to attempt the identification of coordination in each pair of fetal-maternal time series. First magnitude of heart rates and their frequencies studied.
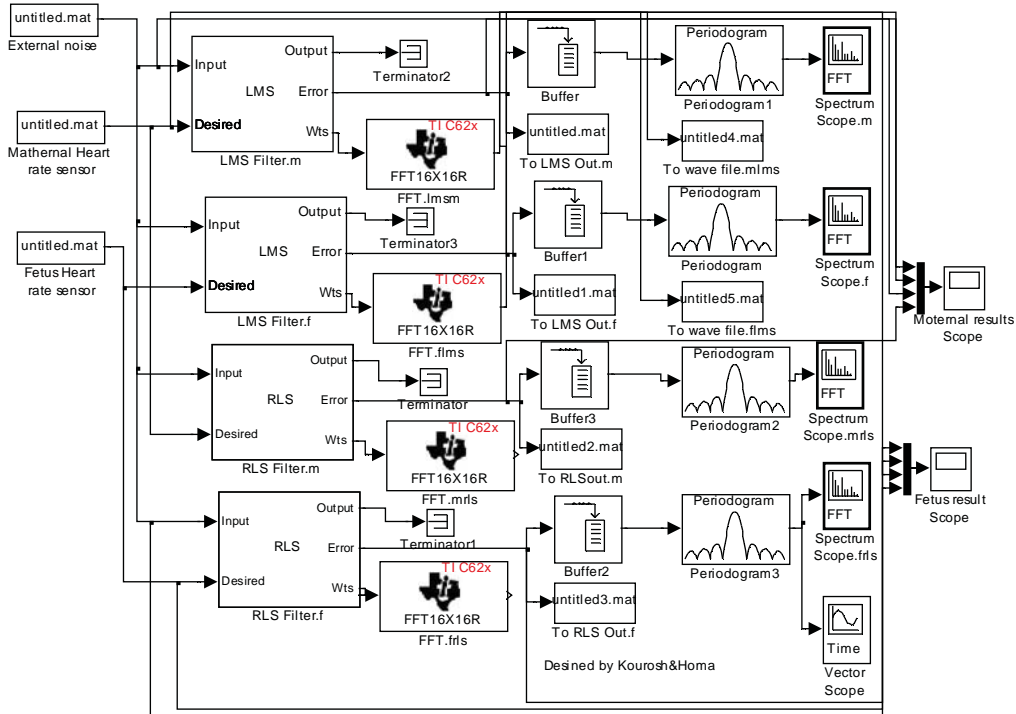


**Figure12**: SIMULINK model of two different used adaptive filter

These were examined for equally spaced peaks and troughs. The frequency distributions also were investigated for uniformity and the ratio of fetal peaks to maternal peaks was noted for all nonuniform distributions identified.

Synchrograms were simulated using the stroboscopic technique: the phases of the fetal R peaks ($\varphi_{mat}$) were studied with respect to m maternal cycles. Compared to the method described above, this representation displays the phase of fetal R peaks within one or more maternal RR interval on a time axis. Horizontal groupings of data points indicate phase synchronization. The number of parallel lines (n) in an epoch of such horizontal groupings embedded in m maternal RR intervals indicates the coupling ratio n:m. Due to pages publication limitation in this paper, time series and phase synchronization graphs and histograms weren't traced.

### 1.2 Statistics

Values are generally expressed as means ± standard deviation (SD). The uniformity of the distribution in the histograms was tested using the Chi square procedure. Differences between the results obtained in the real and surrogate data were tested using the Mann-Whitney U-test or the Chi square test. p-values below 0.05 were considered statistically significant

### 1.3 More information's derived by F-MCG

Fetal magnetocardiography test results have the other diagnosis data. Using F-MCG signals and its analysing the other fails of fetus can be diagnosed and detected. These signals carry many useful data on fetus. One of that are fetal hiccups, tachycardia and etc. Fetal hiccups emerge as early as nine weeks post-conception, being the predominant diaphragmatic movement before 26 weeks of gestation. They are considered as a programmed isometric inspiratory muscle exercise of the fetus in preparation for the post-natal respiratory function, or amanifestation of a reflex circuitry underlying the development of suckling and gasping patterns.

Several studies have investigated the relationship between fetal hiccups and fetal behavioural state. In a systematic study of hiccups in the fetal baboon, Stark et al (1994) bremarked that bouts of hiccups were not associated with transitions in the behavioural state.

Additionally, their temporal features (overall incidence, hiccup rate, bout duration and inter-bout duration) did not vary with the fetal state. Similarly, in the human fetus, van Woerden et al (1989) found no specific relationship between hiccups and fetal behavioural states or movement patterns. Studying the alteration in the fetal hiccup response following vibroacoustic stimulation, Goldkrand and Farkouh (1991) noted that hiccups were absent in all non-reactive results to non-stress test (NST), speculating that hiccup absence in a non-reactive NST may be an indicator of fetal compromise.

Hiccups are generally observed in newborns, while disappearing gradually in infancy.Reportedly, pre-term infants spend up to 2.5% of their time hiccupping. In neonates, hiccups are immediately terminated by the suckling reflex.

F-MCG simulation performed with insert a hiccups noises in the simulation results. This noise added to Simulink model and then recognized again. Figure 12 shows the results.
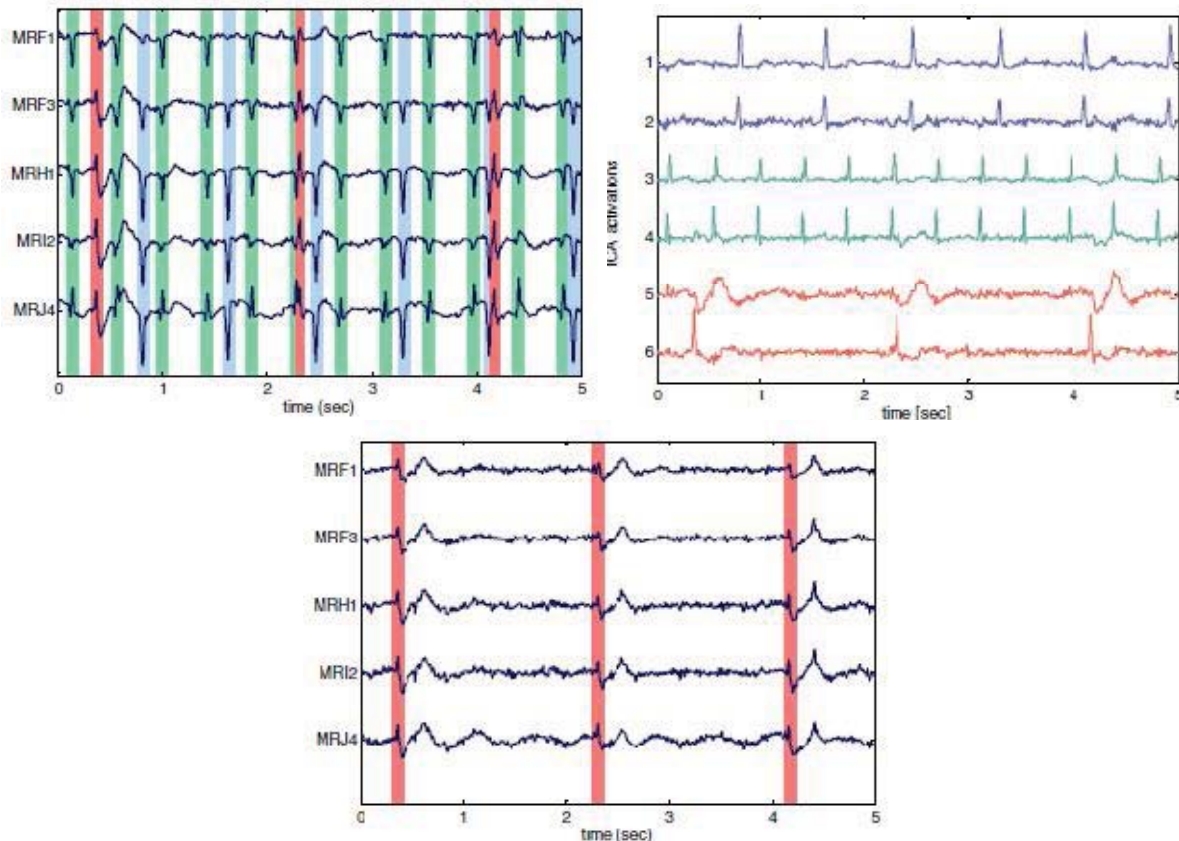


**Figure12.** Channel data and independent component analysis (ICA) decomposition are illustrated for fetus.

In figure 12 derived: (a) Magnetographic data are exemplified for a subset of channels (5 out of 63); fetal hiccup events, fetal cardiac beats and maternal cardiac beats are highlighted. (b) ICA decomposition of the dataset shown in panel (a) is exemplified for a subset of relevant ICs; fetal hiccuping activity is shown in IC5 and IC6, fetal cardiac activity in IC3 and IC4, and maternal cardiac activity in IC1 and IC2. (c) Filtered channel data are shown for a subset of channels, after fetal and maternal cardiac interference is removed by ICA filtering.

### 1.4 Disadvantages of magnetocardiography

In adult cardiography, there are many reasons for preferring the use of the ECG rather than the MCG. An important consideration is the ease of application. For example, if only the heart rate is desired, then the ECG may prove much simpler. The reason is that the measurement of the MCG, at present, is technologically more complicated and requires complex and expensive equipment. Specifically, this includes a SQUID magnetometer, liquid helium, and a low-noise environment. Because of the development of the SQUID technology, a shielded room is no longer needed in magnetocardiography. (In the near future, it seems possible to operate the SQUIDs at the liquid nitrogen temperature which decreases the operational costs considerably.)

## 2 Conclusions

Magnetic field emitted by mother and fetus heart simulated and analyzed in the presented paper. Author using the electric, magnetic and physical given data has been performed simulation in Comsol software. Obtained data transferred to Matlab software and using Simulink and its capability like adaptive filters, noise in the gathered signals cancelled. Pure signals of mother and fetus achieved and analysed. Results shown that mother and fetus heart rate can be recognized, detected and separated. Results verified by signas obtained by Echo/Doppler images and found that there is a good convergences between them. Both signals are in the range of 3e-9 for mother and 2e-11 for fetus. In simulation and calculations signal to noise ratio had a acceptable values.

Based of achieved and analyzed data, author suggested using of F-MCG in diagnosing and monitoring of fetus. Its non invasive and non side effects advantages encourage the doctors and gestation's mother to use of this method.

For adult it need to more study that authors make a comparison between MCG and EKG, results are in the following:

The MCG measures the electric activity of the heart muscle. Therefore, on grounds of cost-effectiveness, if only one of these methods is used when such recordings can be done electrically, the ECG should be used unless there are technical reasons for selecting the MCG (e.g., in screening tests, in patients with skin burns, in recording DC fields, etc.).

The ECG measures the electric potential field, which is a scalar field. Therefore, one measurement at each measurement location is enough. The MCG measures the magnetic field, which is a vector field. Therefore, MCG measurements should provide a vector description - that is, three orthogonal measurements at each measurement location.

In MCG we are interested in the electric activation of the whole cardiac muscle, not only on its anterior surface. Therefore, to compensate the proximity effect, MCG measurements should be done symmetrically both on the anterior and on the posterior side of the thorax. Actually, the posterior measurement of the MCG increases the information especially on the posterior side of the heart, where the sensitivity of all ECG leads is low due to the insulating effect of the lungs. (As noted earlier, in the measurement of the MEG, we are mainly interested in the electric activation of the surface of the brain, the cortex. Therefore a unipolar measurement is more relevant in measuring the MEG.)

On the basis of the existing literature on the MCG, nonsymmetric unipositional measurement seems to give the same diagnostic performance as the mapping of the x component of the magnetic field on the anterior side of the thorax.

A combination of electric and magnetic measurements (i.e., ECG and MCG) gives a better diagnostic performance than either method alone with the same number of diagnostic parameters, because the number of independent measurements doubles.

## 3 References

[1] Takeda, S et al (1992): *Age variation in the upper limit of hearing*. European Journal of Applied Physiology. 65 (5): 403–408. Retrieved on 17 November 2008.

[2] Paul Vitello: *A Ring Tone Meant to Fall on Deaf Ears*. (New York Times article), June 12, 2006.

[3] Nicholas J. Hangiandreou: *AAPM/RSNA Physics Tutorial for Residents: Topics in US*. B-mode US: Basic Concepts and New Technology - Hangiandreou 23 (4): 1019 - RadioGraphics , 2003.

[4] Watson, T: *Therapeutic Ultrasound*, 2006

[5] AIUM.: Journal of ultrasound in medicine features bio effects consensus report, 2006, http://en.wikipedia.org/wiki/Ultrasound

[6] Kourosh Mousavi Takami: *Effects of electromagnetic and electrical fields on human health*. KAHROBA journal (specialized in power electric engineering), 1998, April.

[7] Kourosh Mousavi Takami, Homa Hekmat: *Simulation and Calculation of Magnetic and Thermal Fields of Human using Numerical Method and Robust Soft wares*, The 49th Scandinavian Conference on Simulation and Modeling (SIMS 2008) Oslo, Norway at Oslo University College, October 7th-8th, 2008. ISBN-13: 978-82-579-4632-6.